Geotech Geol Eng (2016) 34:1669–1676
DOI 10.1007/s10706-016-0048-0

TECHNICAL NOTE

Large Deformation Finite Element Analysis of Vane Shear Tests

T. Gupta · T. Chakraborty · K. Abdel-Rahman · M. Achmus

Received: 16 August 2015 / Accepted: 22 June 2016 / Published online: 27 June 2016

Abstract In the present work, three dimensional large deformation elastoplastic finite element (FE) analysis of vane shear test (VST) has been carried out using the coupled Eulerian–Lagrangian (CEL) technique in FE software Abaqus/Explicit. The soil stress–strain response has been simulated using the Mohr–Coulomb constitutive model. The vane is modeled as rigid body in the simulation. The results of CEL simulations have been compared with the laboratory test results to understand the capability of CEL technique in simulating VST through large deformation FE procedure. It is observed that CEL can successfully simulate the laboratory VST. The success of numerical model was verified by comparing torque required at failure in numerical simulation that of laboratory results. The maximum rotation moment obtained from CEL-modelling of VST is lower compared to the experimentally obtained moment whereas the shear stress distributions obtained from VST simulation is reasonable.

Keywords Coupled Eulerian–Lagrangian technique · Finite element analysis · Large deformation analysis · Vane shear test

T. Gupta · T. Chakraborty (✉)
Department of Civil Engineering, Indian Institute of Technology (IIT), Delhi, New Delhi 110 016, India
e-mail: tanusree@civil.iitd.ac.in

T. Gupta
e-mail: tanmayshlok90@gmail.com

K. Abdel-Rahman · M. Achmus
Institute for Geotechnical Engineering (IGtH), Leibniz Universität Hannover, 30167 Hannover, Germany
e-mail: khalid@igth.uni-hannover.de

M. Achmus
e-mail: achmus@igth.uni-hannover.de

1 Introduction

In the last few decades, significant advancement has happened and robust algorithms are developed in different numerical procedures, e.g. coupled Eulerian–Lagrangian (CEL) finite element method, mesh free methods, boundary element method. These numerical methods have been successfully applied in solving challenging boundary value problems in geotechnical engineering—pile penetration analysis (Henke et al. 2011; Dijkstra et al. 2011), spudcan penetration analysis (Gütz et al. 2013) are some examples. Moreover, the CEL method has been used by a number of researchers to investigate the penetration of spudcan foundations in various soil stratigraphies (Qiu and Grabe 2012; Tho et al. 2012, 2013; Pucker et al. 2013; Hu et al. 2014), penetration of cone (Wang et al. 2015; Gupta et al. 2015) and uplift capacity of rectangular plates (Chen et al. 2013). Numerical simulation of common laboratory and field tests not only improve soil characterization for construction projects, but also provide a tool for cross verification

analysis in more complicated boundary value problem. In the present work, one of the most commonly used laboratory tests has been considered for simulation, viz. vane shear test (VST).

The VST is used for calculating the undrained shear strength of cohesive soil (Bjerrum 1972). Figure 1 shows a typical vane and the maximum torque (T_{max}) required to rotate the vane in soil which is used to calculate the undrained shear strength of soil. For interpretation of VST results, it is assumed that soil is isotropic in nature and that the soil fails along the cylindrical failure surface having diameter (D) and height ($L = 2D$) equal to that of vane. The undrained shear strength from field VST $(s_u)_{fv}$ is given by

$$(s_u)_{fv} = \frac{6T_{max}}{7\pi D^3} \quad (1)$$

Bjerrum (1972) however observed that the strength of soft clays measured using VST is significantly higher than the field strength and proposed empirical correction factors to vane shear strength for taking into account of the effect of anisotropy and the rate effect of soil in field. Thus, the mobilized undrained shear strength in VST is given by

$$(s_u)_{design} = \mu_A \mu_R (s_u)_{fv} \quad (2)$$

where μ_A = empirical correction factor for anisotropy of clay which depends on the inclination of slip surface formed in clay due to vane rotation and μ_R = empirical correction factor to consider shear rate.

Numerical simulation of VST in the literature is rather limited. Griffiths and Lane (1990) performed two dimensional and quasi three dimensional finite element analysis of VST considering only tangential movement of material along the blades of vane. Their study concluded that the Eq. (1) represents a very good estimate for cohesive strength of isotropic and non-softening soils. Pérez-Foguet et al. (1999) performed an analysis of the vane test using an Arbitrary Lagrangian–Eulerian formulation within a finite element framework. They analysed the shear stress distributions on the failure surface and presented the dependence of shear band formation on the constitutive model selected. They also mentioned that for usual vane tests, viscous forces are predominant, and the measured shear strength depends mainly on the angular velocity applied. The objectives of the present work are to simulate vane shear test using the coupled Eulerian–Lagrangian technique in the finite element software Abaqus and compare the simulation results with the experimental data. Further, the present study aims to understand the distribution of shear stress along the blades of the vane.

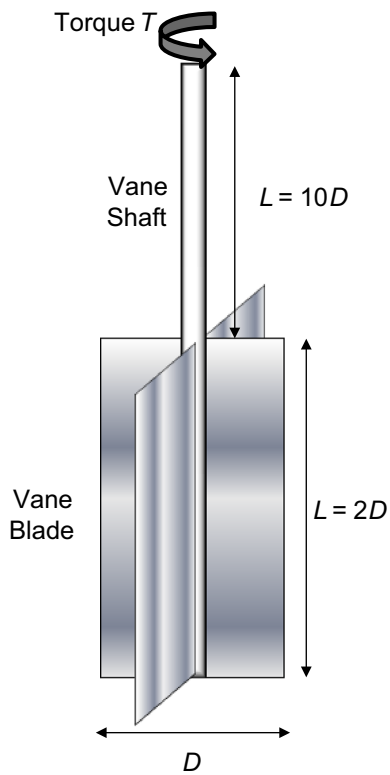

Fig. 1 A typical diagram of vane for vane shear test

2 Numerical Modeling

2.1 Coupled Eulerian–Lagrangian Technique

The Eulerian formulation in Abaqus provides stresses and strains in a convected co-ordinate system as opposed to Lagrangian formulation which provides stresses and strains with respect to a fixed co-ordinate system. In Eulerian analysis, material flows through the elements which are fixed in space and some material may flow out of Eulerian part thus making it excluded from analysis. Thus there is no distortion of mesh in Eulerian part. The material may completely fill the element or may fill a part of it. The part of the

Eulerian element which do not have any material assignments are considered as void in the analysis. The Eulerian volume fraction (EVF) tool is used to assign material in an element. If an element is completely filled with material then its EVF is equal to unity and if there is no material in an element then its EVF is equal to zero. Eulerian part can only be meshed with three dimensional EC3D8R elements from Abaqus library.

The time incrementation in CEL technique is based on operator split of governing equation, which results in traditional Lagrangian phase followed by an Eulerian phase. There is also a check of element deformation after the end of Lagrangian time increment phase in which a tolerance limit is used to determine elements having significant deformation. This check allows elements having very little or no deformation to remain inactive during Eulerian phase.

Problems involving penetration or rotation of Lagrangian part in Eulerian part needs to be dealt with special care as heavy flow of material takes place through the mesh. Hence, a void space needs to be created at Eulerian mesh boundary to account for the flow of material replaced by penetration or rotation. This void space is necessary to track the heave of soil during penetration in VST and also to track the material flow.

2.2 Numerical Modelling of VST

In the present study, numerical simulation of VSTs in cohesive soils has been carried out using the CEL method. Herein, the soil domain and the vane have been modelled as two different parts. The soil domain has been modelled using eight node linear reduced integration Eulerian hexahedral elements (EC3D8R) and the vane has been modelled using eight node linear reduced integration Lagrangian hexahedral elements (C3D8R) along with rigid body constraint having reference point on the axis of vane shaft. Table 1 gives the vane properties used herein. The soil domain considered herein has a diameter of 96 mm and height of 120 mm. It may be noted that 40 mm of soil void is added on top of the soil part which provides space for the movement of soil. The top of vane blade is kept 15 mm inside the soil at the initial stage of the simulation. The details of different mesh sizes which are used in this numerical model for mesh convergence study are given in Table 2. Figure 2 shows a typical finite element mesh for the soil domain and the vane inserted in soil. The stress–strain response of soil is simulated using the Mohr–Coulomb constitutive model and the vane is modelled as a rigid body. In order to replicate the laboratory VST conditions in numerical model, the velocity of nodes at the bottom of the soil domain is kept zero in all active degrees of freedom ($V_x = V_y = V_z = 0$). The outer surface of cylindrical domain is kept constrained from horizontal motion of nodes i.e. x and y directions of velocities have zero value $V_x = V_y = V_z = 0$. A frictional interface is simulated between vane and soil using the penalty contact with coefficient of friction 0.1 considering residual shear strength of clay (Bishop et al. 1971). Initial conditions to define the state of soil are also prescribed which are inherent to CEL technique to assign material in the specified regions of Eulerian part. Initial stresses are defined in the model based on the density of soil. The earth pressure coefficient at rest ($K_0 = 1 - \sin\phi'$) is used to calculate the horizontal stresses at any given depth.

Two types of loading have been applied in this study to account for the rotation of vane and the effect of gravity. The effect of gravity is introduced by specifying an acceleration of 10 m/s^2 in negative z-direction for the material assigned section in the Eulerian part. The second type of loading used in this analysis is the velocity at the reference node which controls the movement of vane in all directions. In this loading definition, a constant velocity of rotation is specified to rotate the vane in soil domain.

Table 1 Vane characteristics and properties

Blade height (mm)	Blade diameter (mm)	Shaft diameter (mm)	Blade thickness (mm)	Young's modulus (GPa)	Poisson's ratio	Density (tonnes/m^3)
25.4	12.7	3.5	0.05	200	0.30	7.75

Table 2 Mesh description for soil domain (VST)

Mesh	Coarse	Medium	Fine
Number of elements in soil domain	109,592	120,204	145,152

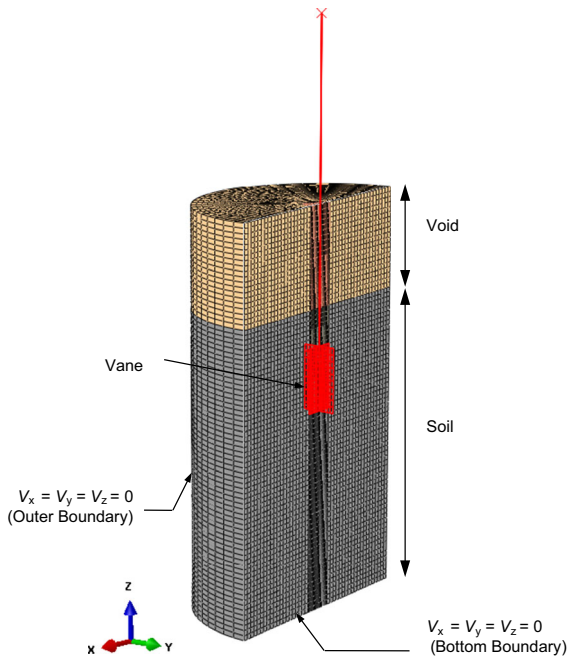

Fig. 2 Typical finite element mesh of vane and the surrounding soil

2.3 Material Model

The soil stress–strain response has been simulated using the Mohr–Coulomb plasticity criterion available in the Abaqus library. It is an elastic perfectly plastic failure criterion to depict the behavior of soil. The yield surface of the Mohr–Coulomb model in the principal stress ($\sigma_1 - \sigma_2 - \sigma_3$) space is given by

$$F = R_{mc}q - p\tan\phi - c = 0 \tag{3}$$

where c is the cohesion, ϕ is the angle of friction of soil, p is the mean stress and q is the deviatoric stress. The parameter R_{mc} defines the shape of the Mohr–Coulomb yield surface in the deviatoric plane (π-plane). Non-associated flow rule is assumed in the analysis with the plastic potential function G_P different from the yield function F, given by

$$G_P = \sqrt{(\varepsilon c_0 \tan\psi)^2 + (R_{mw}q)^2} - p\tan\psi \tag{4}$$

where ψ is the dilation angle, c_0 is the initial cohesion yield stress, ε is the meridional eccentricity and R_{mw} determines the shape of the plastic potential surface in the π-plane. Inside the yield surface, the soil behavior is assumed to be linear elastic with Young's modulus (E) and Poisson's ratio (ν). In simulation of VST, the soil parameters used to model clayey soil are given in Table 3 as obtained from experiments discussed in next section. Herein, the undrained response of soil is modelled by taking Poisson's ratio = 0.49 and pore water is not considered in the current analyses. Small but non zero value of friction and dilation angles are considered to avoid any instability in numerical calculations and cohesion is thus the governing parameter controlling the results.

3 Experimental Study on VST: Laboratory Experiment

Laboratory miniature VST is performed on three soft clay samples of different water contents as given in Table 3 to find the undrained shear strength of clay samples and the residual shear strength. The VST in the laboratory is performed according to ASTM D4648 standards. The vane considered in experiment has a diameter of 12.7 mm and height of 25.4 mm. The diameter of soil sample is taken as 96 mm and height of soil sample is taken as 120 mm. The vane is inserted in soil in such a way that the top of vane is 15–20 mm below the soil surface. Vane is rotated at a speed of 6°/min. This speed of vane rotation is necessary to model the undrained behavior of soil. The vane area ratio, i.e., the ratio of cross sectional area of vane to the area to be sheared of the vane used herein is 13.7 %. The results of VST are presented herein in terms of rotational moment as shown in Fig. 3. Once the soil reaches its peak strength, the speed of rotation is increased to 600°/min to reach the residual strength of clay. It may be observed from the graph that the

Table 3 Soil properties for VST

Soil sample number	Water content (%)	Density (tonnes/m^3)	Young's modulus (MPa)	Poisson's ratio	Friction angle (°)	Dilation angle (°)	Input cohesion strength (kPa)
1	115	1.9	4.0	0.49	1.0	0.85	3.77
2	82	1.9	4.0	0.49	1.0	0.85	10.89
3	45	1.9	4.0	0.49	1.0	0.85	15.41

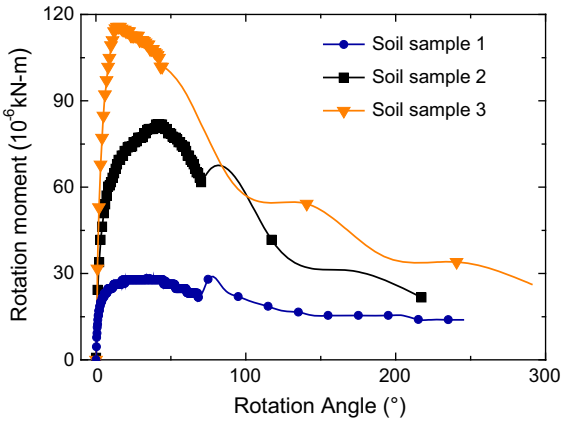

Fig. 3 Experimental results for three different soil samples

peak strength of soil is achieved at different values of rotation angles for three soil types and the failure of soil occurs at this peak strength. This peak state represents the maximum shear strength of soil and is used for calculating the mobilized field shear strength of soil with the use of correction factor defined in Eqs. (2).

4 Numerical Simulation of VST

4.1 Calibration

Figure 4a shows the rotational moment calculated from the simulations of VST for different mesh sizes. The finest mesh has been used for all the simulations reported herein. Also, three different speeds of rotation are taken into consideration to prove the independency of numerical model on the speed of rotation. The rotation speed has been defined as angular velocity using the predefined field applied at the reference point of rigid body constraint and maintained constant throughout the analysis.

Three vane rotation speeds have been considered, e.g., 6, 8 and 10°/s for comparison purpose. Figure 4b shows the effect of vane rotation speed on the rotation moment of the vane. It is observed that results are also independent of vane rotation velocity. It may be noted here that the material model used herein is strain rate independent. The velocity of rotation is used herein for analyzing the response of VST for three different types of clay. To decrease the CPU time, a velocity of 10°/s is taken in all analyses.

It may be noted that as per ASTM D2573, the standard vane rotation speed is 0.1–0.2°/s. Herein, higher vane rotation speed is used for purely numerical reasons because the undrained response of cohesive soil is modelled using Poisson's ratio and vane speed has no effect on the results.

5 Results and Discussions

Table 4 presents the comparison between experimental and numerical results. The results for rotation moment obtained from numerical analysis is compared to the rotation moment obtained from the experiments for the equal value of numerical input cohesion strength and experimental undrained shear strength. The obtained maximum rotation moment from CEL-modelling of VST (23.42×10^{-6} kN m) is about 80 % compared to the experimentally obtained moment (28.30×10^{-6} kN m) for soil sample number 1. This reduction in obtained rotation moment is found to be consistent for all the soil samples (Table 4). In order to find out the reasons for this reduction in the numerical results, the distribution of the mobilized shear stress along the failure planes is investigated.

Figure 5a shows the distribution of the mobilized shear stress along a vertical path of vane edge in the soil domain for three different soil samples. The

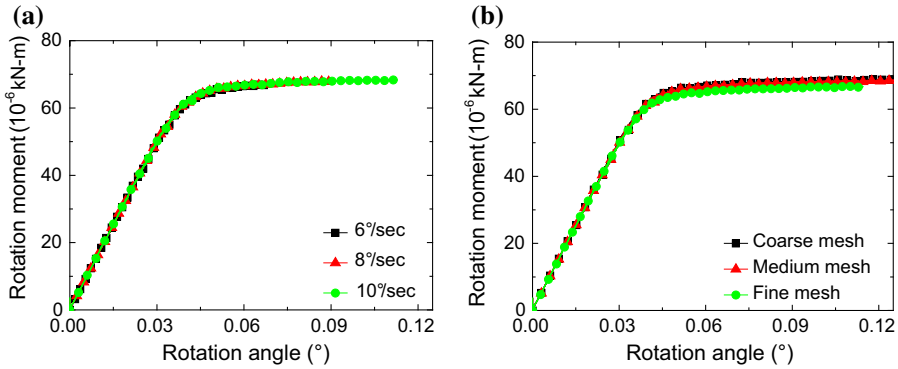

Fig. 4 Effect of **a** rotational velocities of vane and **b** mesh size of soil domain on the rotational moment of vane

Table 4 Comparison between experimental and numerical analysis for VST

Soil sample number	Experimental		Numerical	
	Maximum rotation moment × 10^{-6} (kN m)	Undrained shear strength (kPa)	Input cohesion strength (kPa)	Maximum rotation moment × 10^{-6} (kN m)
1	28.30	3.77	3.77	23.42
2	81.75	10.89	10.89	67.67
3	115.69	15.41	15.41	95.76

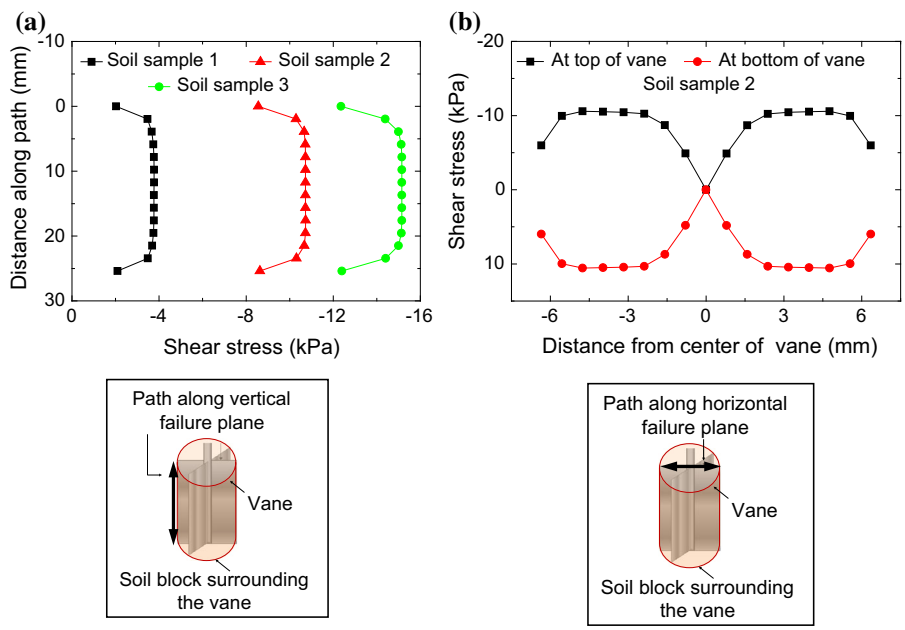

Fig. 5 Plot of shear stress distribution **a** *vertical path* adjacent to vane in soil domain and **b** *horizontal path* at *top* of vane in soil domain for three different samples

results show almost a constant shear stress distribution along the edge of the vane, i.e. 10.89 kPa for sample number 2, which decreases towards the outer corners of the vane. It is observed that the shear stress values are almost identical to the input cohesion (c_u) values given in Table 4. Figure 5b shows the distribution of

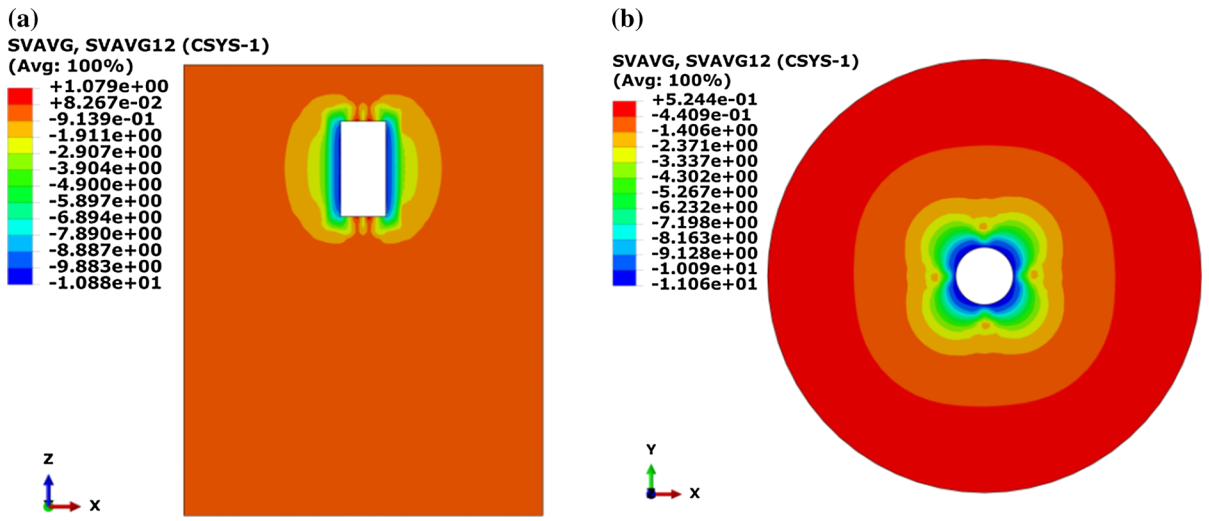

Fig. 6 Shear stress distribution in soil **a** along a *vertical plane* and **b** a *horizontal plane* along the vane for soil sample 2

shear stress along top and bottom horizontal failure planes of soil. These plots show that the mobilized shear stress is almost constant on the middle part of vane blades, i.e. 10.89 kPa for sample number 2, and equal to the undrained shear strength which is also 10.89 kPa. Also the shear stress magnitudes are equal to zero at the center of the vane showing that no shearing of soil takes place at that point.

Figure 6a, b show contours for shear stresses in soil along a vertical cross section and a horizontal cross section at mid height of vane, respectively for sample number 2. The empty space in center has radius equal to that of vane. The contour shows that the shear stress distribution is fairly uniform along the circumferential path and is equal to the input undrained cohesion strength in the numerical model. Both the vertical and the horizontal contours are symmetric with respect to the vane which is reasonable.

It is observed from the VST results that the rotational moment obtained from the numerical modelling is lesser than that obtained experimentally which may be attributed to the difference between the shear stress distributions obtained from numerical simulation compared to the assumed one adopted in Eq. (1) and also, the use of rate independent material properties. Also according to Bjerrum (1972) the correction factor for undrained shear strength from VST was required to incorporate the rate effects only, however, the results obtained in the present work show that the non-constant distribution of shear stresses along the surface of the failed soil mass also requires a correction.

6 Conclusions

A numerical model is developed in order to understand the undrained shear strength response of a saturated cohesive soil subjected to VST. The CEL analysis procedure is used to simulate the large deformation of soil during the analysis. The CEL method is very successful in representing the effect of large deformation on stress strain response of soil domain.

The soil is modelled using the Mohr–Coulomb failure criteria and the response of soil till failure is studied. It is conferred from the results that the Eq. (1) gives a higher value of cohesive strength of clay from the measured rotation moment in laboratory test. The consideration of stress distribution pattern in numerical model shows that the assumptions have significant effect on the cohesive strength of soil as calculated from maximum rotation moment.

The current study may be used as a benchmark which has established that the CEL analysis procedure is a very powerful tool in numerical Geotechnical engineering to analyze the problems involving large scale deformation. Thus, the complexity of soil structure interaction is no longer an obstacle in finite element analysis with problems involving large deformation.

Acknowledgments This work has been carried out with scholarship funded by DAAD for Mr. Tanmay Gupta for a period of 6 months. This work is a result of collaboration between Institute for Geotechnical Engineering, LUH, Germany and Department of Civil Engineering, IIT Delhi, India.

References

Abaqus/Explicit User's Manual, Version 6.11. Dassault Systèmes Simulia Corporation, Providence, Rhode Island, USA, 2011

ASTM D2573 Standard test method for field vane shear test in cohesive soil. West Conshohoken, Pa, 2008

ASTM D4648 Standard test method for laboratory miniature vane shear test for saturated fine-grained clayey soil. West Conshohoken, Pa, 2003

Bishop AW, Green GE, Garga VK, Andresen A, Brown JD (1971) New ring shear apparatus and its application to the measurement of residual strength. Geotechnique 21(4):273–328

Bjerrum L (1972) Embankments on soft ground. In: Proceedings of the ASCE conference on performance of earth-supported structures 1972, Purdue University, vol 2, pp 1–54

Chen Z, Tho KK, Leung CF, Chow YK (2013) Influence of overburden pressure and soil rigidity on uplift behavior of square plate anchor in uniform clay. Comput Geotech 52:71–81

Dijkstra J, Broere W, Heeres OM (2011) Numerical simulation of pile installation. Comput Geotech 38:612–622

Griffiths PV, Lane PA (1990) Finite element analysis of shear vane test. Comput Struct 37(6):1105–1116

Gupta T, Chakraborty T, Abdel-Rahman K, Achmus M (2015) Large deformation finite element analysis of static cone penetration test. Indian Geotech J. doi:10.1007/s40098-015-0157-3

Gütz P, Peralta P, Abdel-Rahman K, Achmus M (2013) Numerical investigation of spudcan footing penetration in layered soil. In: Proceedings of 5th international conference on computational methods in marine engineering 2013, Hamburg, Germany

Henke S, Qiu G, Grabe J (2011) Application of a coupled Eulerian Lagrangian approach on geomechanical problems involving large deformations. Comput Geotech 38:30–39

Hu P, Wang D, Cassidy MJ, Stanier SA (2014) Predicting the resistance profile of a spudcan penetrating sand overlying clay. Can Geotech J 51:1151–1164

Pérez-Foguet A, Ledesma A, Huerta A (1999) Analysis of the vane test considering size and time effects. Int J Numer Anal Meth Geomech 23(5):383–412

Pucker T, Bienen B, Henke S (2013) CPT based prediction of foundation penetration in siliceous sand. Appl Ocean Res 41:9–18

Qiu G, Grabe J (2012) Numerical investigation of bearing capacity due to spudcan penetration in sand overlying clay. Can Geotech J 49(12):1393–1407

Tho KK, Leung CF, Chow YK, Swaddiwudhipong S (2012) Eulerian finite element technique for analysis of jack-up spudcan penetration. Int J Geomech 12(1):64–73

Tho KK, Leung CF, Chow YK, Swaddiwudhipong S (2013) Eulerian finite element simulation of spudcan–pile interaction. Can Geotech J 50(6):595–608

Wang D, Bienen B, Nazem M, Tian Y, Zheng J, Pucker T, Randolph MF (2015) Large deformation finite element analyses in geotechnical engineering. Comput Geotech 65:104–114